Supporting Information

Formation and Scrolling Behavior of Metal Fluoride and Oxyfluoride Nanosheets

Roshini Ramachandran,[‡] Darrah Johnson-McDaniel,[‡] and Tina T. Salguero[*]

Department of Chemistry, The University of Georgia, 140 Cedar Street, Athens, GA 30602 USA

Contents:

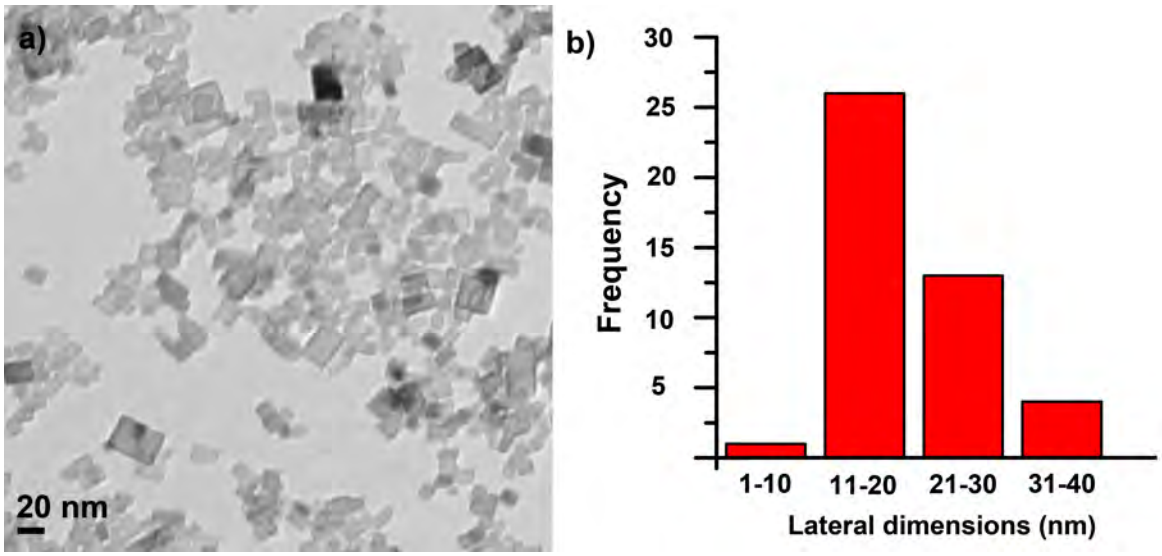

Figure S1. Size distribution of the rectangular CaF_2 nanosheets: a) Representative TEM image. b) Histogram of nanosheet lateral dimensions; the average size is 17-22 nm.

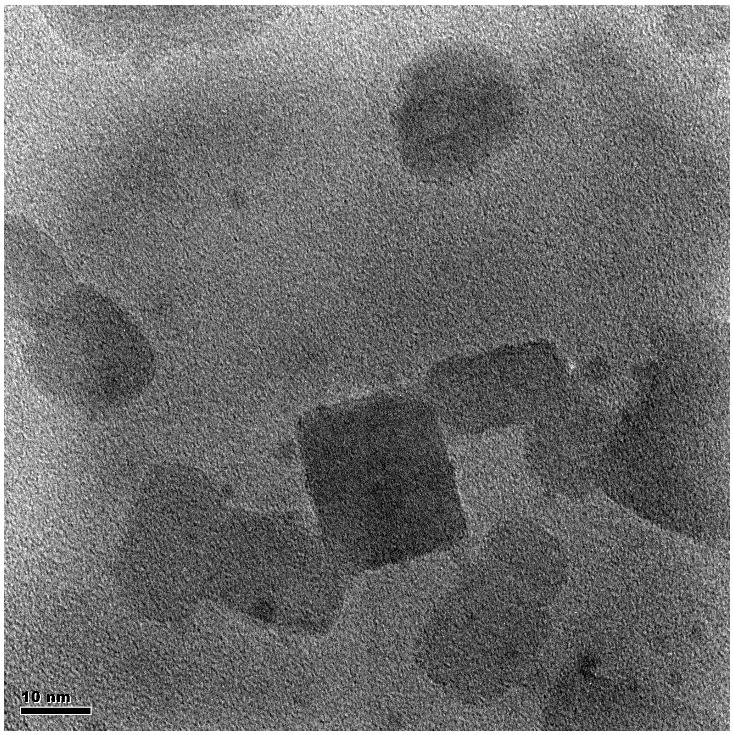

Figure S2. HRTEM imaging showing the mixed morphology of the CaF_2 nanoproduct: rectangular nanosheets plus irregular nanoparticles.

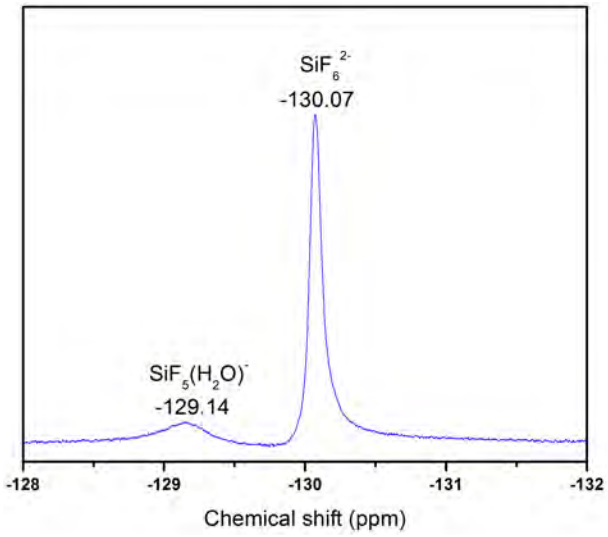

Figure S3. Solution-state ^{19}F NMR of the $CaSi_2$ + HF(aq) reaction mixture.

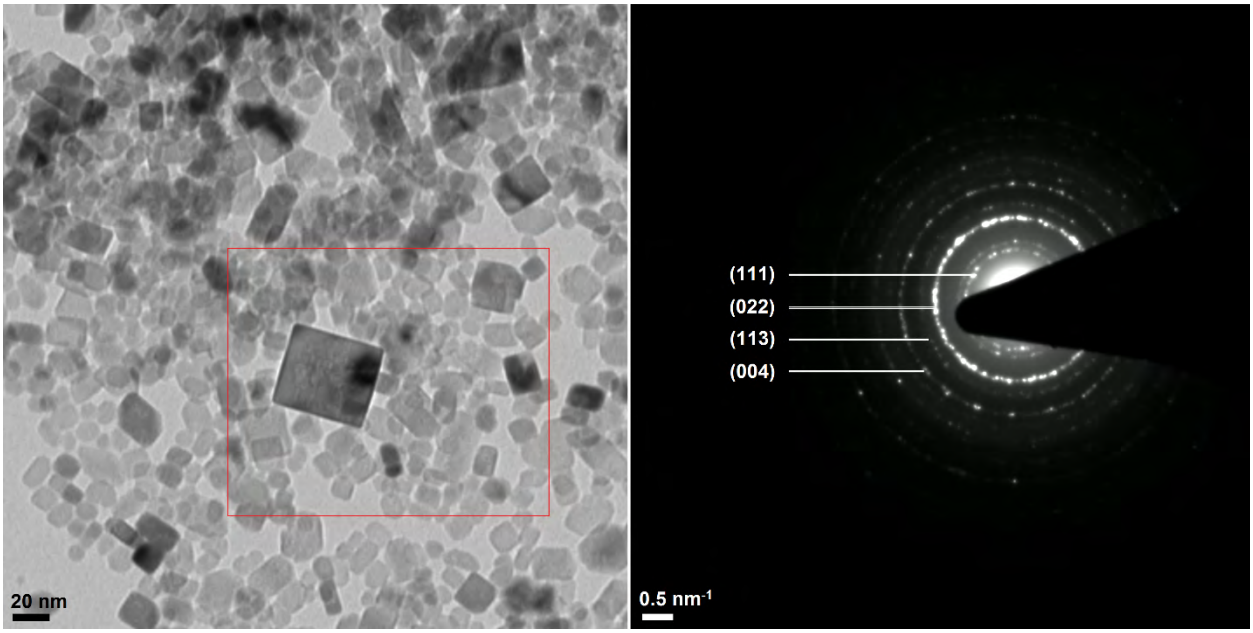

Figure S4. SAED of the CaF_2 nanosheets showing polycrystalline rings indexed to CaF_2

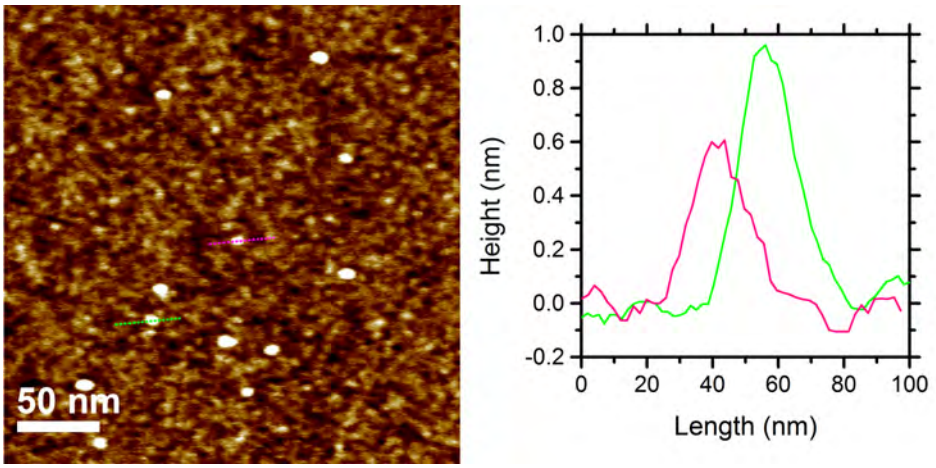

Figure S5. AFM data for CaF_2 nanosheets; their thicknesses range from 0.6 to 1 nm.

Table S1. Scherrer analysis of CaF_2 nanosheets and $LaF_{3-2x}O_x$ nanoscrolls (shape parameter 0.9).

	Peak used	2-theta (degrees)	FWHM	Particle size (nm)	Average size (nm)
CaF_2 nanosheets	CaF_2 (111)	32.97	0.4154	24.20	22.37
	CaF_2 (220)	55.20	0.5018	21.68	
	CaF_2 (311)	65.87	0.5410	21.23	
$LaF_{3-2x}O_x$ nanoscrolls	LaF_3 (002)	28.02	0.9942	9.99	22.84
	LaF_3 (111)	32.12	0.3060	32.78	
	LaF_3 (300)	51.00	0.4146	25.76	

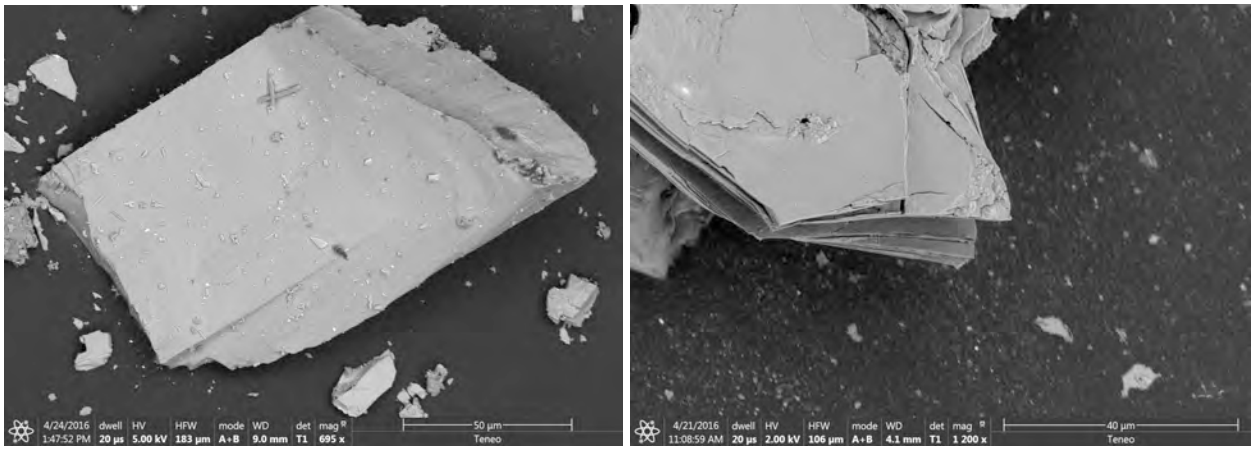

Figure S6. SEM images of $CaSi_2$ before reacting with HF (left) and partially reacted $CaSi_2$ after reaction with HF (right) showing lateral cracking due to partial removal of Ca^{2+} by F^-.

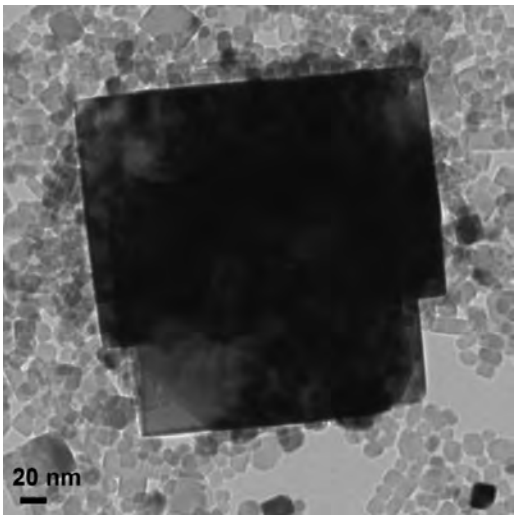

Figure S7. TEM image of a sparse CaF_2 platelet formed during the reaction of $CaSi_2$ + HF(aq).

Table S2. Relative intensities of the ^{19}F resonances from the CaF_2 nanosheet sample.

δ_{iso} (ppm)	Relative intensity
-108.1	83.3%
-82.8	5.0%
-122.6	2.1%
-127.4	4.5%
-133.4	5.1%

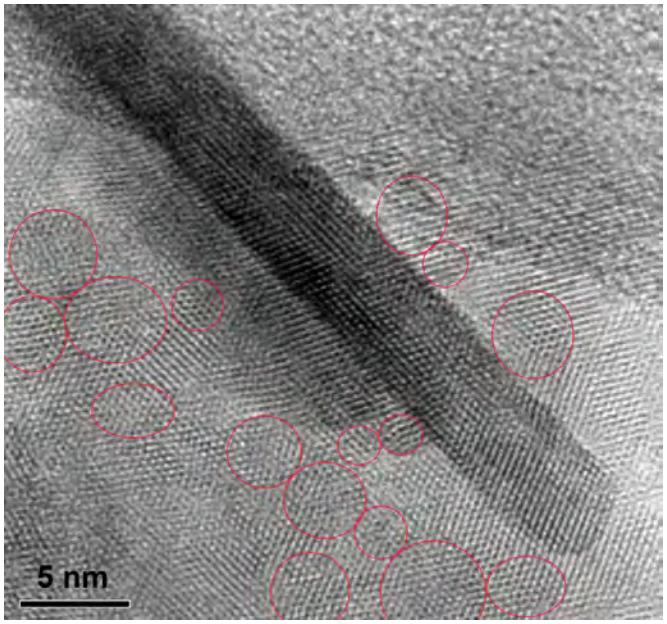

Figure S8. Circled clusters of nanoparticles surrounding a $LaF_{3-2x}O_x$ nanoscroll.

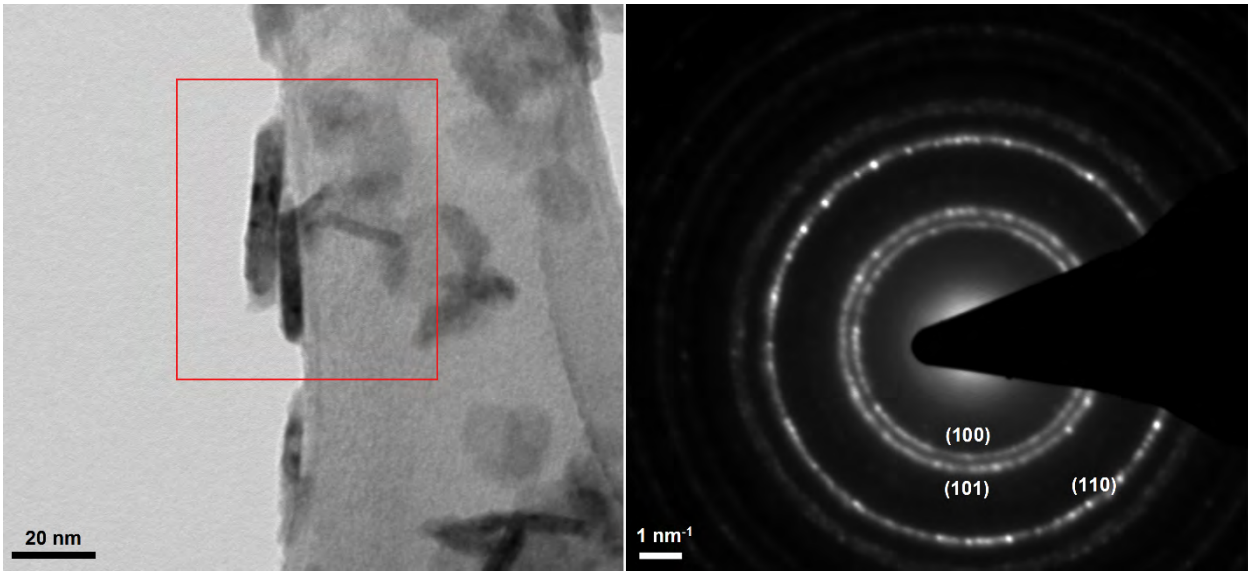

Figure S9. SAED of the $LaF_{3-2x}O_x$ nanoscrolls showing polycrystalline rings indexed to LaF_3.

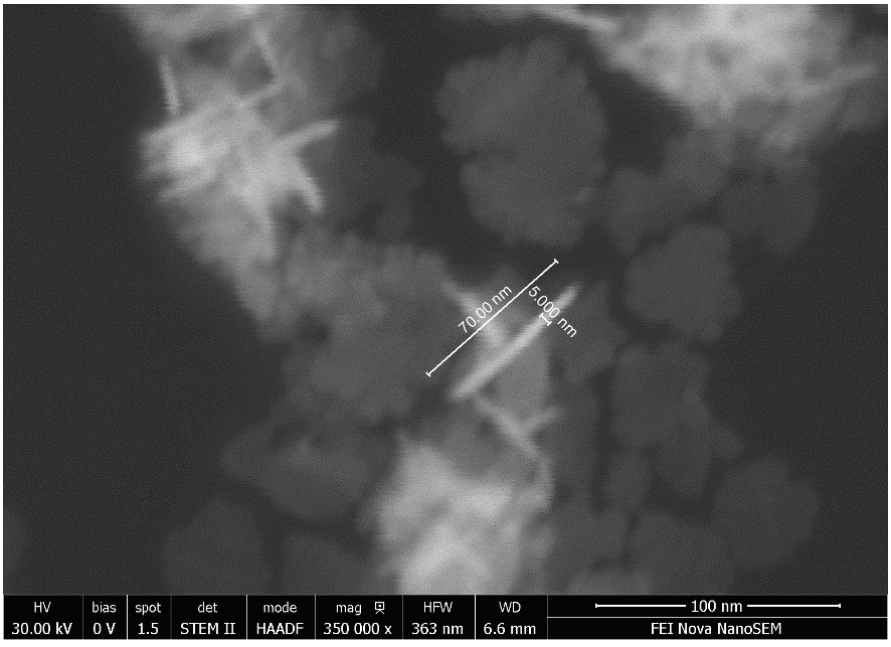

Figure S10. Measurement of $LaF_{3-2x}O_x$ nanoscroll diameter from STEM image.

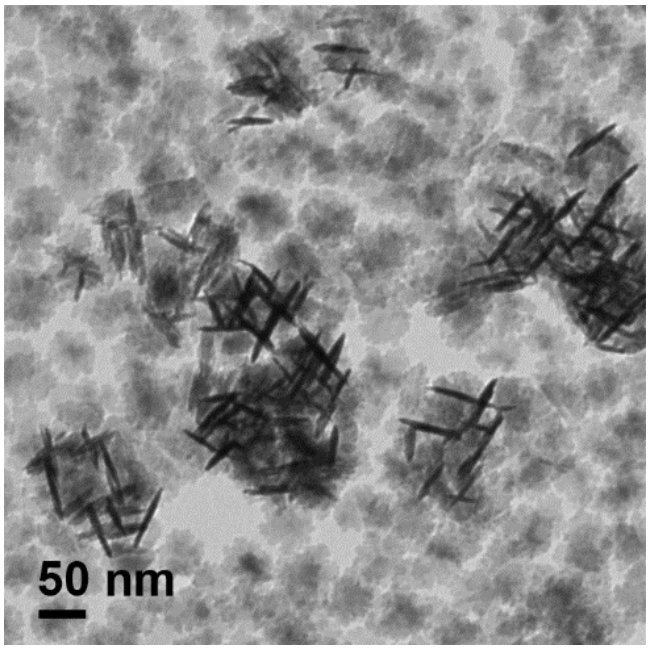

Figure S11. TEM image of the $LaF_{3-2x}O_x$ nanoscrolls using $La(CF_3SO_3)_3$.

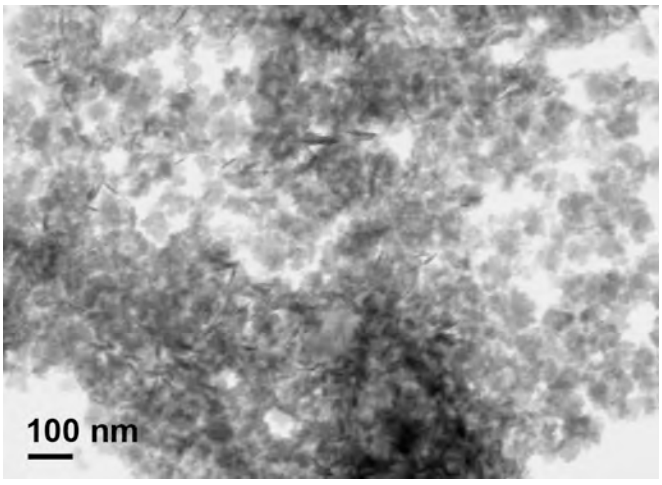

Figure S12. STEM image of the $LaF_{3-2x}O_x$ nanoscrolls using $LaBr_3$.

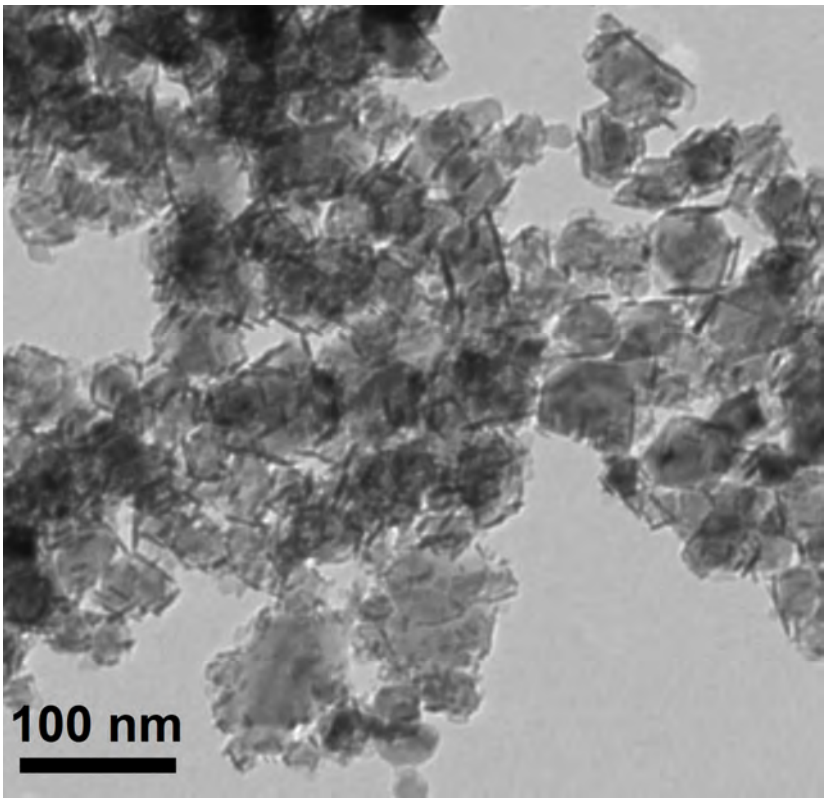

Figure S13. TEM image of partially scrolled nanosheets using sub-stoichiometric amount of $La(CF_3SO_3)_3$.

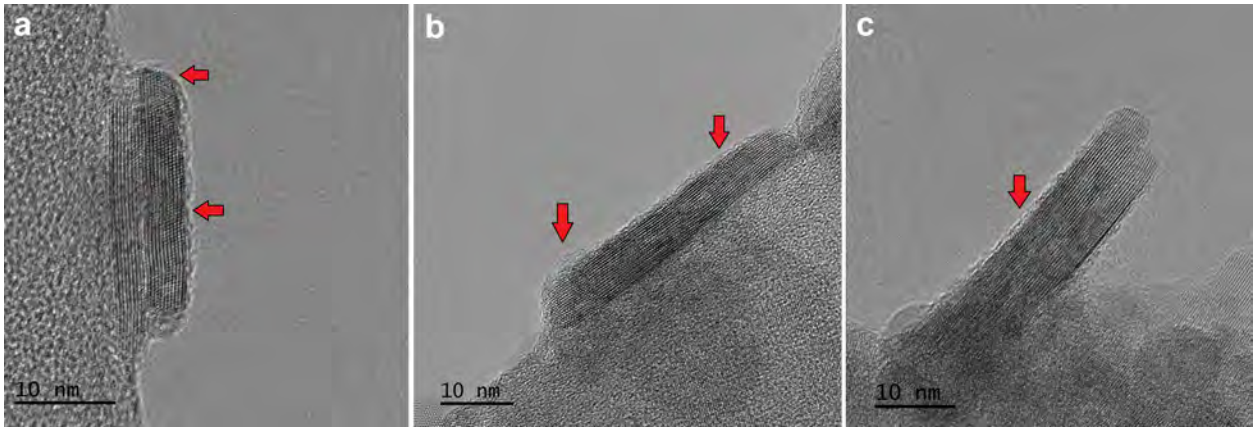

Figure S14. HRTEM images of partially rolled (a, c) and fully rolled nanoscrolls (b) highlighting their rolled-up nature and open ends. Arrows indicate areas where lattice fringes change from overlap due to curvature upon rolling.

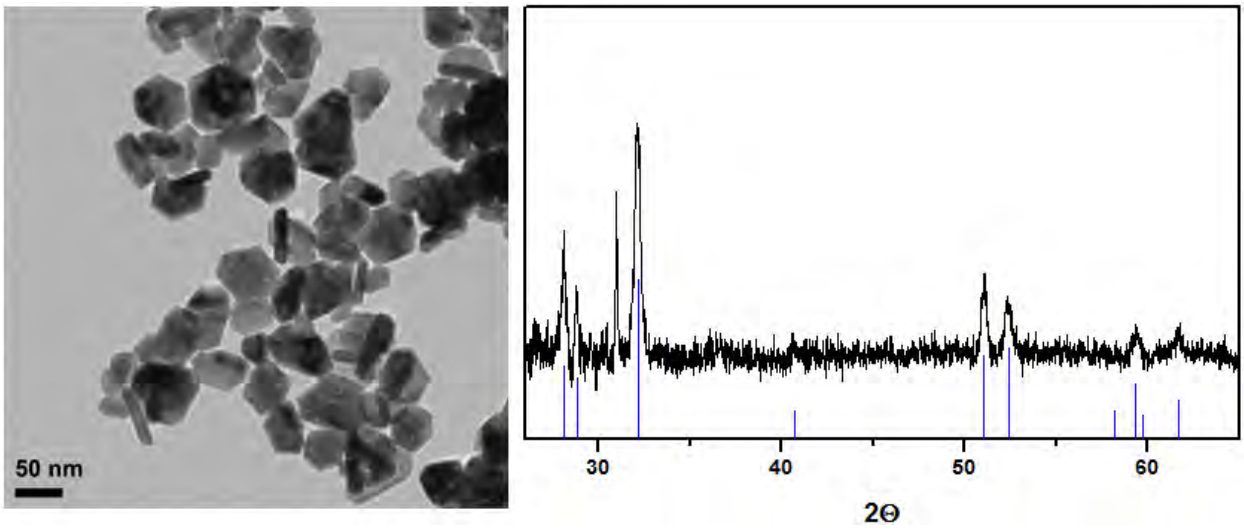

Figure S15. a) TEM image of LaF_3 nanocrystals obtained from the hydrothermal reaction of CaF_2 nanosheets with $LaCl_3$ b) Experimental PXRD pattern (black) with reference pattern (blue sticks) matching hexagonal LaF_3 (ICDD no. 04-005-4417).

Table S3. Quantitative EDS measurements on the $LaF_{3-2x}O_x$ nanoscrolls.

Element	Series	Atomic %
La	K-series	26.79
F	K-series	52.38
O	K-series	20.38
Ca	K-series	0.44

Table S4. Peak values for XPS measurements.

Sample	Element	Peak positions			
		1s	2s	2p	3d
$LaF_{1.955}O_{0.76}$ nanoscrolls	La	--	--	--	842.47 859.35 862.97
	F	--	--	705.01 706.28	--
	O	531.97 532.82	--	--	--
	Si	--	--	107.78 111.38	--